Science
AAAS

Phosphoproteomic Analysis Identifies Grb10 as an mTORC1 Substrate That Negatively Regulates Insulin Signaling

Yonghao Yu, *et al.*

Science **332**, 1322 (2011);
DOI: 10.1126/science.1199484

Science (print ISSN 0036-8075; online ISSN 1095-9203) is published weekly, except the last week in December, by the American Association for the Advancement of Science, 1200 New York Avenue NW, Washington, DC 20005.

proteins, which are likely the most important effects of mTOR inhibitors to consider in their clinical use (Fig. 4G). Our findings also support the idea (*30*, *31*) that concomitant IGF-1 receptor inhibition may improve the anticancer efficacy of mTOR inhibitors. Finally, the discovery of Grb10 as an mTORC1 substrate validates our approach and suggests that the other potential downstream effectors that we identified may also serve as starting points for new areas of investigation in mTOR biology.

References and Notes

1. M. Laplante, D. M. Sabatini, *J. Cell Sci.* **122**, 3589 (2009).
2. R. Zoncu, A. Efeyan, D. M. Sabatini, *Nat. Rev. Mol. Cell Biol.* **12**, 21 (2011).
3. R. J. Dowling, I. Topisirovic, B. D. Fonseca, N. Sonenberg, *Biochim. Biophys. Acta* **1804**, 433 (2010).
4. P. L. Ross *et al.*, *Mol. Cell. Proteomics* **3**, 1154 (2004).
5. C. C. Thoreen *et al.*, *J. Biol. Chem.* **284**, 8023 (2009).
6. J. H. Choi *et al.*, *EMBO Rep.* **3**, 988 (2002).
7. C. H. Jung *et al.*, *Mol. Biol. Cell* **20**, 1992 (2009).
8. I. G. Ganley *et al.*, *J. Biol. Chem.* **284**, 12297 (2009).
9. N. Hosokawa *et al.*, *Mol. Biol. Cell* **20**, 1981 (2009).
10. O. J. Shah, Z. Wang, T. Hunter, *Curr. Biol.* **14**, 1650 (2004).
11. A. Y. Choo, S. O. Yoon, S. G. Kim, P. P. Roux, J. Blenis, *Proc. Natl. Acad. Sci. U.S.A.* **105**, 17414 (2008).
12. M. E. Feldman *et al.*, *PLoS Biol.* **7**, e38 (2009).
13. L. R. Pearce, D. Komander, D. R. Alessi, *Nat. Rev. Mol. Cell Biol.* **11**, 9 (2010).
14. C. K. Yip, K. Murata, T. Walz, D. M. Sabatini, S. A. Kang, *Mol. Cell* **38**, 768 (2010).
15. J. E. Hutti *et al.*, *Nat. Methods* **1**, 27 (2004).
16. J. Mok *et al.*, *Sci. Signal.* **3**, ra12 (2010).
17. H. E. Polson *et al.*, *Autophagy* **6**, 506 (2010).
18. R. Parker, U. Sheth, *Mol. Cell* **25**, 635 (2007).
19. K. Nykamp, M. H. Lee, J. Kimble, *RNA* **14**, 1378 (2008).
20. A. Huber *et al.*, *Genes Dev.* **23**, 1929 (2009).
21. J. Coller, R. Parker, *Cell* **122**, 875 (2005).
22. L. J. Holt, K. Siddle, *Biochem. J.* **388**, 393 (2005).
23. M. Charalambous *et al.*, *Proc. Natl. Acad. Sci. U.S.A.* **100**, 8292 (2003).
24. F. M. Smith *et al.*, *Mol. Cell. Biol.* **27**, 5871 (2007).
25. L. Wang *et al.*, *Mol. Cell. Biol.* **27**, 6497 (2007).
26. A. Morrione *et al.*, *J. Biol. Chem.* **274**, 24094 (1999).
27. X. R. Cao *et al.*, *Sci. Signal.* **1**, ra5 (2008).
28. L. S. Harrington *et al.*, *J. Cell Biol.* **166**, 213 (2004).
29. L. R. Pearce *et al.*, *Biochem. J.* **431**, 245 (2010).
30. K. E. O'Reilly *et al.*, *Cancer Res.* **66**, 1500 (2006).
31. X. Wan, B. Harkavy, N. Shen, P. Grohar, L. J. Helman, *Oncogene* **26**, 1932 (2007).

Acknowledgments: We thank members of the Sabatini Lab for helpful discussion, especially B. Joughin, G. Bell, H. Keys, K. Birsoy, N. Kory, C. Thoreen, J. Claessen, and D. Wagner for assistance with technical or conceptual aspects of this project. This work was supported by the National Institutes of Health (grants CA103866 and AI47389 to D.M.S.; ES015339, GM68762, and CA112967 to M.B.Y.), Department of Defense (W81XWH-07-0448 to D.M.S.), the W.M. Keck Foundation (D.M.S.), LAM Foundation (D.M.S.), Dana-Farber Cancer Institute (N.S.G, J.M), the International Fulbright Science and Technology Award (J.R.), and American Cancer Society (S.A.K.). D.M.S. is an investigator of the Howard Hughes Medical Institute. Torin1, the drug used in this paper, is part of a Whitehead-DFCI patent application on which N.S.G. and D.M.S. are inventors. Shared reagents are subject to a Materials Transfer Agreement.

Supporting Online Material

www.sciencemag.org/cgi/content/full/332/6035/1317/DC1
Materials and Methods
Figs. S1 to S12
Tables S1 to S4
References

25 October 2010; accepted 22 April 2011
10.1126/science.1199498

Phosphoproteomic Analysis Identifies Grb10 as an mTORC1 Substrate That Negatively Regulates Insulin Signaling

Yonghao Yu,[1] Sang-Oh Yoon,[1]* George Poulogiannis,[2] Qian Yang,[1,3] Xiaoju Max Ma,[1]† Judit Villén,[1]‡ Neil Kubica,[1]§ Gregory R. Hoffman,[1] Lewis C. Cantley,[2] Steven P. Gygi,[1]‖ John Blenis[1]‖

The evolutionarily conserved serine-threonine kinase mammalian target of rapamycin (mTOR) plays a critical role in regulating many pathophysiological processes. Functional characterization of the mTOR signaling pathways, however, has been hampered by the paucity of known substrates. We used large-scale quantitative phosphoproteomics experiments to define the signaling networks downstream of mTORC1 and mTORC2. Characterization of one mTORC1 substrate, the growth factor receptor–bound protein 10 (Grb10), showed that mTORC1-mediated phosphorylation stabilized Grb10, leading to feedback inhibition of the phosphatidylinositol 3-kinase (PI3K) and extracellular signal–regulated, mitogen-activated protein kinase (ERK-MAPK) pathways. Grb10 expression is frequently down-regulated in various cancers, and loss of Grb10 and loss of the well-established tumor suppressor phosphatase PTEN appear to be mutually exclusive events, suggesting that Grb10 might be a tumor suppressor regulated by mTORC1.

The evolutionarily conserved Ser-Thr protein kinase mammalian target of rapamycin (mTOR) functions as the core catalytic component of two structurally and functionally distinct signaling complexes. mTOR complex 1 (mTORC1) regulates protein translation, autophagy, and cell growth, whereas mTOR complex 2 (mTORC2) regulates the actin cytoskeleton and cell survival (*1*–*3*). mTORC1 and mTORC2 respond to upstream inputs such as growth factors, energetic status, and amino acid levels (*3*), but relatively few downstream targets of mTOR have been identified.

Misregulated mTOR activity is a common feature of most cancers (*1*), but clinical trials evaluating the mTORC1 selective inhibitor rapamycin as an anticancer agent have met with limited success (*2*). Rapamycin resistance has emerged as a major challenge to its clinical use (*4*) and is caused in part by feedback loops that activate the phosphatidylinositol 3-kinase (PI3K) and extracellular signal–regulated, mitogen-activated protein kinase (ERK-MAPK) signaling pathways in rapamycin-treated cells through poorly understood mechanisms (*5*, *6*). Identifying substrates of mTORC1 and mTORC2 will be important for understanding how mTOR signals downstream and for defining components of feedback loops involved in rapamycin resistance.

We performed two sets of large-scale, quantitative phosphoproteomics experiments to characterize the signaling network downstream of mTOR (Fig. 1 and figs. S1 to S3). The first stable isotope labeling with amino acids in cell culture (SILAC) experiment (Rapa screen) was performed using *Tsc2*$^{-/-}$ mouse embryonic fibroblasts (MEFs) [see supporting online material (SOM) text for detailed description of the screen]. We identified 4484 and 6832 unique phosphorylation sites on 1615 and 1866 proteins from two biological replicate experiments, respectively (table S1 and databases S1 and S2).

[1]Department of Cell Biology, Harvard Medical School, Boston, MA 02115, USA. [2]Division of Signal Transduction, Beth Israel Deaconess Medical Center, Boston, MA 02215, USA. [3]Harvard School of Dental Medicine, Boston, MA 02115, USA.

*Present address: Department of Cancer and Cell Biology, University of Cincinnati, College of Medicine, Cincinnati, OH 45267, USA.
†Present address: Department of Research Oncology Diagnostics, Genentech Inc., 1 DNA Way, South San Francisco, CA 94080, USA.
‡Present address: Department of Genome Sciences, University of Washington, Seattle, WA 98195, USA.
§Present address: Developmental and Molecular Pathways, Novartis Institutes for Biomedical Research, Cambridge, MA 02139, USA.
‖To whom correspondence should be addressed. E-mail: Steven_gygi@hms.harvard.edu (S.P.G); john_blenis@hms.harvard.edu (J.B.)

Several hundred peptides corresponding to 85 and 147 proteins in the two replicates (database S3 and fig. S1) were determined to contain rapamycin-sensitive phosphorylation sites (defined as phosphorylated peptides in control cells whose abundance were more than twice that in samples from rapamycin-treated cells). Many known effectors of the canonical mTORC1 signaling pathway were identified in the down-regulated population, including p70S6K, 4EBP1/2, Akt1s1 (PRAS40), rpS6, eIF4B, eIF4G1, and GSK3β (table S2 and Fig. 1, C and D). A representative identification of the known rapamycin-sensitive phosphorylation sites on rpS6 is shown in Fig. 1B. In addition, the identification of many kinases, for example, unc-51–like kinase 1 (ULK1), in the down-regulated proteins provides potential points for signal integration and crosstalk (table S2) [see SOM text and table S3 for Gene Ontology (GO) analysis and detailed discussion of the hits].

Rapamycin is an allosteric inhibitor that only partially inhibits mTORC1 signaling and has no effect on the activity of mTORC2 under short-term treatment conditions (*2*). In contrast, adenosine triphosphate (ATP)–competitive mTOR inhibitors block the activity of both mTORC1 and mTORC2 (*1*). To identify rapamycin-insensitive mTORC1, and mTORC2 substrates, we used the mTOR inhibitor Ku-0063794 and performed a second SILAC experiment (Ku screen) (Fig. 1, A and C, and fig. S1). In this experiment, 100 proteins were determined to contain down-regulated phosphopeptides after Ku-0063794 treatment (database S3 and table S2) (see SOM text for detailed discussion).

One of the enriched GO classes of hits in the Rapa screen is the receptor protein tyrosine kinase (RTK) signaling pathway ($P = 0.01$, table S3), suggesting that mTORC1 might modulate its upstream regulators by altering the activities of RTKs. In particular, phosphorylation of S501 and S503 on the growth factor receptor–bound protein 10 (Grb10) was strongly inhibited by a 2-hour rapamycin treatment (Fig. 2A, fig. S4A, and table S2). The intensity of a triply phosphorylated Grb10 peptide (T76, S96, and S104) also decreased after rapamycin treatment (table S2).

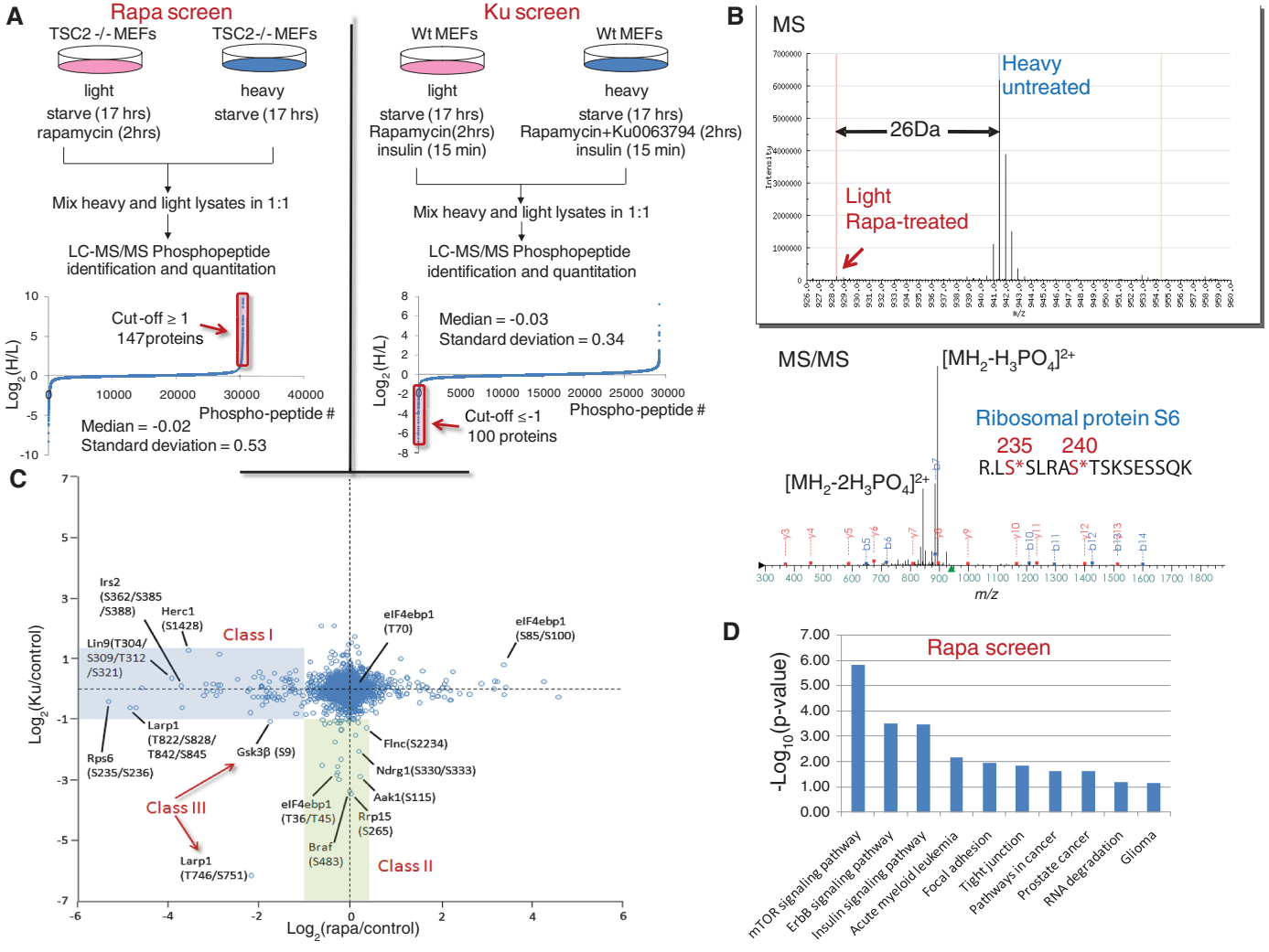

Fig. 1. Sample preparation and data analysis for quantitative phosphoproteomic profiling of the mTOR downstream signaling networks. (**A**) Schematics of the two SILAC mass spectrometry experiments are shown with a plot highlighting the ratio distribution of phosphopeptides identified in each screen (see data summary in table S1). Note that most of the phosphopeptides have a ratio of 1:1 between the light and heavy populations and hence have a value close to 0 on a Log_2 axis. Proteins with down-regulated phosphorylation in each screen are highlighted in the red box. (**B**) Typical mass spectrometry (MS) and tandem mass spectrometry (MS/MS) spectra in which LS*SLRAS*TSKSESSQK from ribosomal protein S6 (S235 and S240) was identified as a rapamycin-sensitive phosphopeptide. The light and heavy peptides differ by 26 daltons, corresponding to two labeled Lys and one labeled Arg in this particular peptide. (**C**) Quantitative differences between the rapamycin-sensitive and insensitive mTOR downstream phosphorylation events. Phosphopeptides identified in both screens were extracted and their corresponding treatment/control ratios (see table S1 for treatment conditions) were plotted on a Log_2 scale. Log_2(treatment/control) ≤ −1 is considered to be down-regulated (see SOM text for detailed discussion). (**D**) The top 10 pathways enriched in the down-regulated phospho-proteins identified in the Rapa screen.

We developed a phospho-specific antibody (fig. S5, A and B) and found that rapamycin treatment induced rapid dephosphorylation of Grb10 at S501 and S503 (Fig. 2B). Grb10 phosphorylation was also decreased in *Tsc2*$^{-/-}$ MEFs deprived of amino acids (Fig. 2C). To determine whether S501 and S503 of Grb10 can be phosphorylated by other kinases, we treated *Tsc2*$^{-/-}$ cells with staurosporine, a broad-spectrum kinase inhibitor that, however, does not suppress mTOR activity (*7*). No change in the phosphorylation of Grb10 was observed (Fig. 2D). S6K activity was inhibited by staurosporine treatment, as shown by a complete loss of rpS6 phosphorylation, suggesting that Grb10 was directly phosphorylated by mTORC1 rather than by S6K.

In wild-type (WT) MEFs, insulin or serum stimulation increased Grb10 phosphorylation in a rapamycin-sensitive manner (Fig. 2E). Akt inhibition also reduced Grb10 and S6 phosphorylation. Grb10 S503 can be phosphorylated by ERK in vitro (*8*). Inhibition of the ERK-activating kinase MEK with AZD6244 abolished phosphorylation of ERK but had no effect on phosphorylation of Grb10 (Fig. 2E), indicating that phosphorylation of S501 and S503 on Grb10 is not mediated by ERK in vivo. All other mTOR catalytic inhibitors tested, including LY294002, NVP-BEZ235, torin, and pp242 (*9*), also completely abolished Grb10 phosphorylation (Fig. 2F).

To examine a potential interaction between Grb10 and the mTOR complexes in vivo, we expressed hemagglutinin (HA)–tagged Grb10 with Myc-tagged raptor or rictor in human embryonic kidney (HEK) 293T cells. Grb10 interacted with raptor, but not rictor, indicating that Grb10 is a binding partner of mTORC1, but not mTORC2 (Fig. 3A). Grb10 was also phosphorylated by recombinant mTOR at S501 and S503 in vitro (Fig. 3B).

Grb10 was much more abundant in *Tsc2*$^{-/-}$ and *Tsc1*$^{-/-}$ MEFs than in their wild-type counterparts (Fig. 3C and fig. S5C), and the initial loss of Grb10 phosphorylation as a result of rapamycin treatment was followed by a decrease in Grb10 abundance and a smaller decrease in the amount of Grb10 mRNA (Fig. 3D). Exposure to a proteosome inhibitor MG-132 suppressed rapamycin-induced Grb10 protein degradation (fig. S5D). These results show that mTORC1 functions to promote accumulation of Grb10 both transcriptionally and posttranslationally. Depletion of the mTORC1 component raptor also led to decreased abundance of Grb10 protein (Fig. 3E). Furthermore, long-term treatment with mTOR catalytic inhibitors led to reduced levels of Grb10 in *Tsc2*$^{-/-}$ MEFs (fig. S5E), *Tsc1*$^{-/-}$ MEFs (fig. S5F), and HeLa cells (fig. S5G).

To explore whether Grb10 S501 and S503 phosphorylation contributed to its stabilization and high expression, we transfected WT Grb10, Grb10-S501A-S503A (AA), and Grb10-S501D-S503D (DD) into HEK293T cells. Exogenous WT and DD Grb10 proteins were expressed in similar amount, but the AA mutant of Grb10 was less abundant, perhaps due to protein instability (Fig. 3F). To confirm this result, we generated *Tsc2*$^{-/-}$ MEFs stably expressing the HA-tagged Grb10-DD. Long-term rapamycin treatment of these cells decreased amounts of the endogenous, WT Grb10 but had no effect on the abundance of the DD mutant protein (Fig. 3G). This result appears not to result from protein overexpression, because in *Tsc2*$^{-/-}$ cells expressing HA-tagged WT Grb10, rapamycin treatment decreased the abundance of both the endogenous

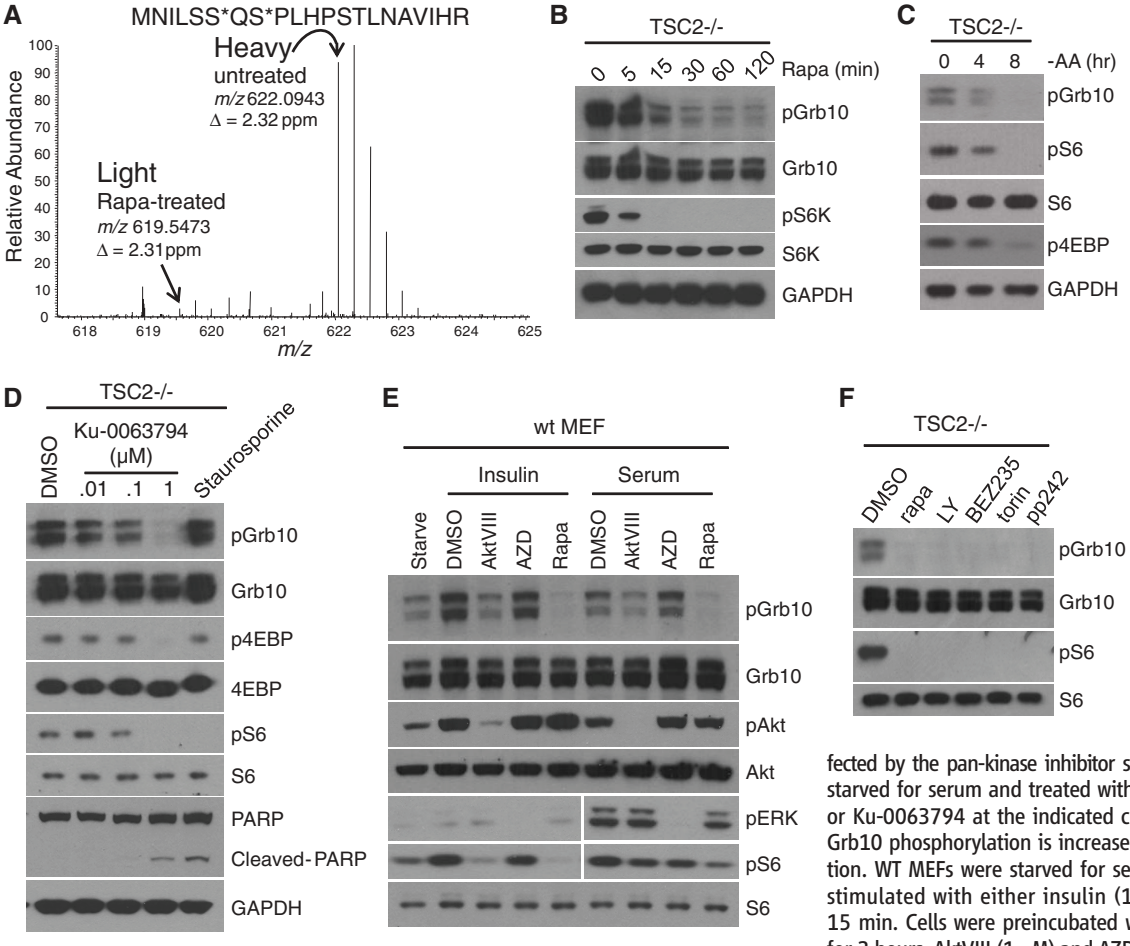

Fig. 2. Sensitivity of phosphorylation of Grb10 at S501 and S503 to rapamycin inhibition. (**A**) Identification of a doubly phosphorylated, rapamycin-sensitive Grb10 peptide (MNILSS*QS*PLHPSTLNAVIHR; asterisk indicates the site of phosphorylation at S501 and S503). (**B**) Phosphorylation of Grb10 at S501 and S503 shows rapamycin sensitivity in vivo. *Tsc2*$^{-/-}$ cells were starved for serum and treated with 20 nM rapamycin for the indicated times. (**C**) Phosphorylation of Grb10 at S501 and S503 is sensitive to amino acids withdrawal. *Tsc2*$^{-/-}$ cells were serum-deprived in Dulbecco's modified Eagle's medium (DMEM) overnight and then transferred to a media of DMEM minus amino acids for the indicated times. (**D**) Phosphorylation of Grb10 at S501 and S503 is not affected by the pan-kinase inhibitor staurosporine. *Tsc2*$^{-/-}$ cells were starved for serum and treated with either 100 nM staurosporine or Ku-0063794 at the indicated concentrations for 2 hours. (**E**) Grb10 phosphorylation is increased upon growth factor stimulation. WT MEFs were starved for serum overnight and then were stimulated with either insulin (100 nM) or serum (10%) for 15 min. Cells were preincubated with the indicated compounds for 2 hours. AktVIII (1 μM) and AZD (AZD6244, 5 μM) are specific inhibitors of Akt and MEK, respectively. Rapa (rapamycin) was used at 20 nM. (**F**) Grb10 phosphorylation at S501 and S503 is sensitive to various mTOR kinase inhibitors. *Tsc2*$^{-/-}$ cells were serum-starved and treated with the indicated compounds for 2 hours. The concentrations of the compounds were Rapa (rapamycin), 20 nM; LY (LY294002), 20 μM; BEZ235 (NVP-BEZ235), 500 nM; torin, 100 nM; and pp242, 1 μM. Phosphorylation levels in this figure were measured with phospho-specific antibodies against Grb10 (S501 and S503), S6K (T389), S6 (S235 and S236), Akt (S473), 4EBP (T37 and T46) and ERK1/2 (T202 and Y204).

and ectopically expressed Grb10 (fig. S5H). These data support a critical role for mTORC1 in stabilizing Grb10 through phosphorylation of the S501 and S503 residues. It is important to note that phospho-Akt levels still increased in these cells (Fig. 3G), likely resulting from increased insulin receptor substrate 1 (IRS1) levels after prolonged rapamycin treatment.

Grb10 functions as a negative regulator of insulin signaling. In Grb10 null mice, PI3K-Akt pathway hyperactivation was observed in insulin-sensitive tissues (*10*, *11*). We therefore examined the possibility that mTORC1-mediated Grb10 phosphorylation and accumulation activated a negative feedback loop from mTORC1 to the PI3K-Akt pathway. The PI3K-Akt and ERK-MAPK pathways were both refractory to insulin or insulin-like growth factor (IGF) stimulation in *Tsc2*$^{-/-}$ cells, as a result of constitutively elevated mTORC1 signaling (*5*, *6*). In contrast, phosphorylation of both Akt and ERK was increased in Grb10-depleted cells deprived of serum or stimulated with insulin or IGF (Fig. 4A and fig. S6A). Conversely, overexpression of Grb10 in HEK293 cells suppressed activation of PI3K (fig. S6B) by inhibiting insulin receptor–dependent phosphorylation of IRS and its subsequent recruitment of PI3K (fig. S6, C and D) (*12*). Knockdown of Grb10 in *Tsc2*$^{-/-}$ MEFs to a level close to that in WT cells did not completely restore the sensitivity of PI3K to insulin stimulation (fig. S6E), suggesting that additional mechanisms (e.g., lower IRS levels in *Tsc2*$^{-/-}$ MEFs) contribute to the feedback inhibition (fig. S6F). Our data complement the previous findings and suggest that activation of mTORC1-S6K promotes negative feedback inhibition of PI3K through a two-pronged mechanism: first, mTORC1-S6K–mediated phosphorylation and degradation of a positive regulator of PI3K signaling, IRS (*6*, *13*, *14*); second, mTORC1-mediated phosphorylation and accumulation of a negative regulator of PI3K signaling, Grb10.

We next asked whether PI3K activation in Grb10-depleted cells would promote survival against stress-induced apoptosis. In response to either staurosporine or etoposide, reduced caspase 3 cleavage was observed in Grb10 knockdown cells compared with that of control cells, indicating that Grb10 depletion is sufficient to protect cells from apoptosis (Fig. 4B and fig. S6G). Because rapamycin can protect cells from energy

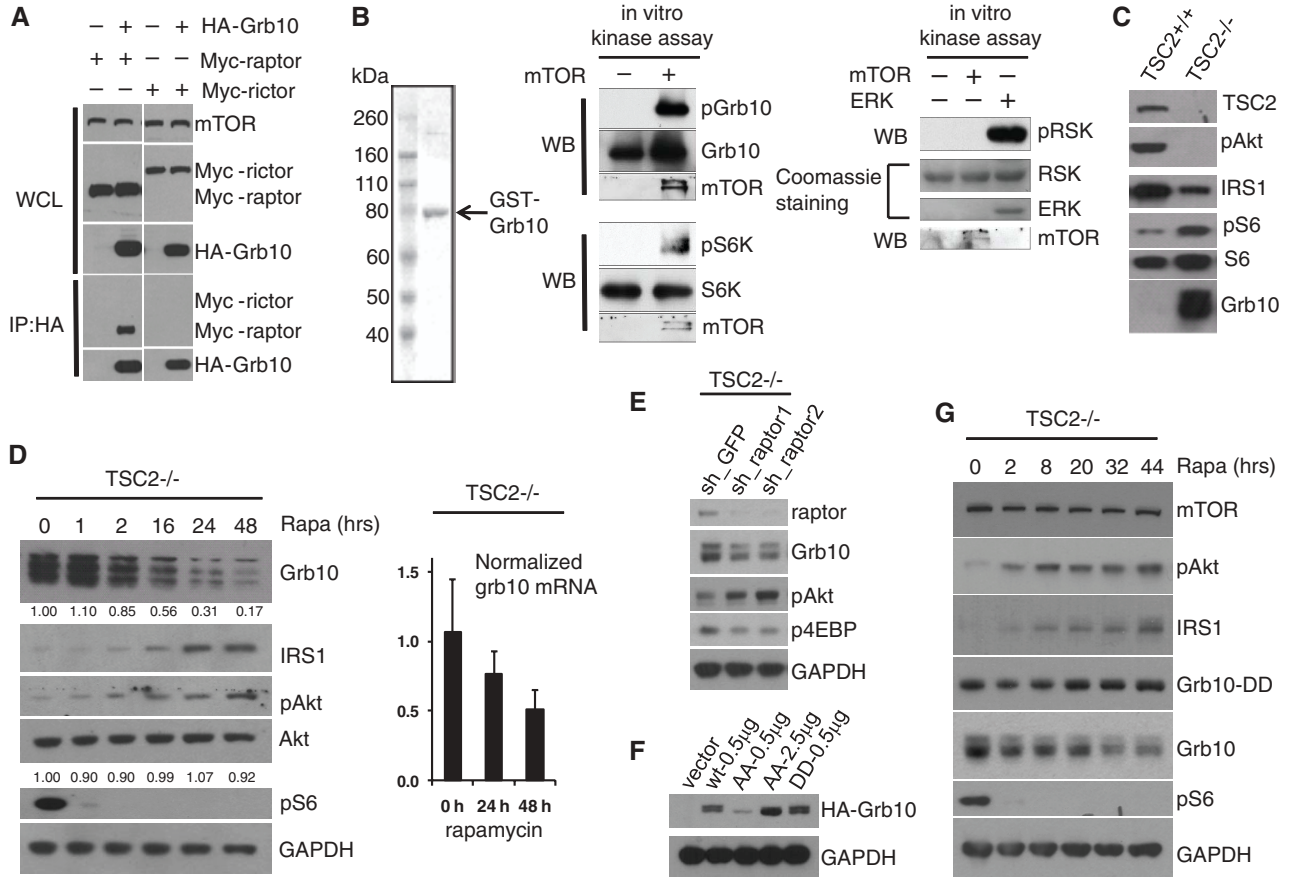

Fig. 3. Effect of mTOR-mediated phosphorylation to promote stability of Grb10. (**A**) Grb10 interacts with raptor, but not rictor. HA-tagged Grb10 was transfected with Myc-raptor or Myc-rictor into HEK293T cells. Cells were lysed in lysis buffer A, and the lysates were subjected to immunoprecipitation using antibody to HA conjugated beads. Raptor and rictor were probed with an antibody against the Myc-tag. WCL, whole cell lysates. (**B**) Grb10 is phosphorylated by mTOR in vitro. Recombinant GST-Grb10 was prepared from bacteria and was incubated with recombinant mTOR in vitro. Phosphorylation of Grb10 at S501 and S503 was detected by using the phospho-specific antibody against these two sites. S6K and ribosomal protein S6 kinase (RSK) were used as the positive and negative controls, respectively, and the experiments were performed in parallel with the mTOR-Grb10 in vitro kinase assay. WB, Western blotting. (**C**) Grb10 is highly overexpressed in *Tsc2*$^{-/-}$ cells. (**D**) Long-term rapamycin treatment leads to Grb10 degradation in *Tsc2*$^{-/-}$ cells. Grb10 protein expression levels inversely correlated with Akt activity. mRNA level was determined using quantitative reverse transcription polymerase chain reaction based on three biological replicate experiments. (**E**) Knockdown of raptor in *Tsc2*$^{-/-}$ cells decreased Grb10 protein level. Cells were starved overnight, and the lysates were probed with the antibodies indicated. (**F**) S501A-S503A mutant is unstable compared with the WT or the S501D-S503D mutant. The indicated amount of DNA was transfected into HEK293T cells. (**G**) Rapamycin failed to induce degradation of the S501D-S503D mutant. S501D-S503D mutant (DD) was stably expressed in *Tsc2*$^{-/-}$ cells, and cells were treated with 20 nM rapamycin for the indicated times. Endogenous Grb10 was detected using an antibody that preferentially recognizes mouse Grb10, whereas the Grb10 DD mutant (of human origin) was detected using an antibody to HA. Phosphorylation levels in this figure were measured with phospho-specific antibodies against Grb10 (S501 and S503), S6K (T389), RSK (T573), Akt (S473), and 4EBP (T37 and T46).

stress-induced death (*15*), these results provide additional possible explanations for the cytostatic rather than cytotoxic effects of rapamycin in some cancers and suggest that a complete understanding of the feedback inhibition control will be critical in designing combination therapies involving rapamycin analogs.

Comprehensive meta-analysis of published microarray data revealed that the abundance of *GRB10* was decreased in many tumor types compared with that in normal tissue counterparts (Fig. 4C). Given that loss of Grb10 results in activation of the PI3K-Akt pathway (Fig. 4A), we performed correlation analysis and found that there was a significant ($P < 0.05$) negative correlation between *GRB10* and *PTEN* expression (Fig. 4, D and E). This correlation was only observed in tumor samples but not in normal tissue controls (Fig. 4E). *PIK3CA* mutations and *PTEN* loss are mutually exclusive in breast cancer (*16*), suggesting that increased abundance of phosphatidylinositol 3,4,5-trisphosphate (PIP_3) resulting from of genetic alteration of either *PIK3CA* or *PTEN* relieves selective pressure targeting the other gene. Similarly, loss of Grb10, which results in PI3K activation, might provide the cells with growth and survival advantages that are redundant with respect to PTEN loss-of-function, suggesting that Grb10 might be a tumor suppressor that is regulated by mTORC1. These data point to the prospect of targeting Grb10 stability in cancer therapy.

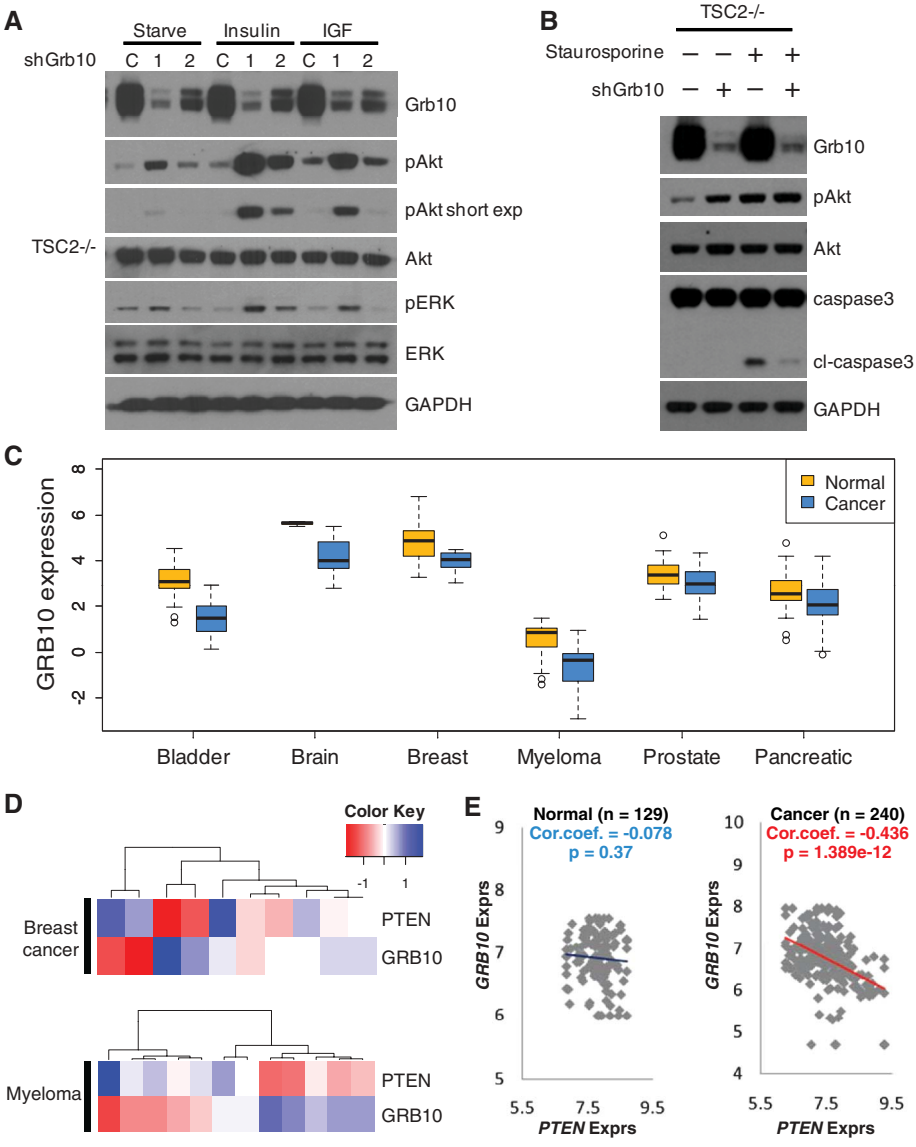

Fig. 4. Grb10 is involved in the feedback inhibition loop from mTORC1 to PI3K and ERK-MAPK, and *GRB10* mRNA expression is decreased in abundance in many cancers and is negatively correlated with *PTEN* expression. (**A**) Knockdown of Grb10 in *Tsc2*$^{-/-}$ cells resulted in PI3K and ERK-MAPK hyperactivation after insulin or IGF stimulation. C, shGFP; 1, shGrb10 #1; 2, shGrb10 #2. Phosphorylation levels were measured against Akt (S473) and ERK1/2 (T202 and Y204). (**B**) Knockdown of Grb10 in *Tsc2*$^{-/-}$ cells protected cells against apoptosis. Grb10 knockdown and control cells were starved overnight and then treated with 100 nM staurosporine for 5 hours to induce apoptosis. Phosphorylation levels were measured against Akt (S473). (**C**) Box plots indicating that *GRB10* expression is significantly lower in many tumor types compared with their corresponding normal tissues. (Only the tumor types that showed significantly lower *GRB10* expression in cancer versus normal in at least three independent microarray data sets are included; $P < 0.01$, Log-rank test.) (**D**) Heat maps indicating a strong negative correlation between *GRB10* and *PTEN* expression in myelomas and breast carcinomas. Low levels of *GRB10* expression rarely occurred in tumors that also showed low levels of *PTEN* expression. The *z* scores (from −1 to +1) of the normalized expression values for the corresponding cancer data sets in (C) are shown. Red, lower expression compared to mean (white). Blue, higher expression compared to mean (white). (**E**) Scatter plots comparing the expression levels of *GRB10* and *PTEN* in the normal and tumor samples, collected from six different tissue types indicated in (C). The negative correlation between *GRB10* and *PTEN* expression is evident in the tumor but not in the corresponding normal samples.

References and Notes

1. D. R. Alessi, L. R. Pearce, J. M. García-Martínez, *Sci. Signal.* **2**, pe27 (2009).
2. A. Y. Choo, J. Blenis, *Cell Cycle* **8**, 567 (2009).
3. X. M. Ma, J. Blenis, *Nat. Rev. Mol. Cell Biol.* **10**, 307 (2009).
4. T. F. Cloughesy *et al.*, *PLoS Med.* **5**, e8 (2008).
5. A. Carracedo *et al.*, *J. Clin. Invest.* **118**, 3065 (2008).
6. O. J. Shah, Z. Wang, T. Hunter, *Curr. Biol.* **14**, 1650 (2004).
7. A. Y. Choo, S. O. Yoon, S. G. Kim, P. P. Roux, J. Blenis, *Proc. Natl. Acad. Sci. U.S.A.* **105**, 17414 (2008).
8. P. Langlais *et al.*, *Biochemistry* **44**, 8890 (2005).
9. D. A. Guertin, D. M. Sabatini, *Sci. Signal.* **2**, pe24 (2009).
10. M. Charalambous *et al.*, *Proc. Natl. Acad. Sci. U.S.A.* **100**, 8292 (2003).
11. L. Wang *et al.*, *Mol. Cell. Biol.* **27**, 6497 (2007).
12. M. A. Lim, H. Riedel, F. Liu, *Front. Biosci.* **9**, 387 (2004).
13. A. Tzatsos, K. V. Kandror, *Mol. Cell. Biol.* **26**, 63 (2006).
14. K. E. O'Reilly *et al.*, *Cancer Res.* **66**, 1500 (2006).
15. A. Y. Choo *et al.*, *Mol. Cell* **38**, 487 (2010).
16. L. H. Saal *et al.*, *Cancer Res.* **65**, 2554 (2005).

Acknowledgments: We thank members of the Blenis and Gygi laboratories for critical discussion. This work was supported by a postdoctoral fellowship from the Tuberous Sclerosis Alliance (grant ID-146 to Y.Y.), and NIH grants GM051405 and CA46595 (J.B.), HG3456 (S.P.G.), and R00CA140789 (J.V.). J.B. is an Established Investigator of the LAM Foundation. A provisional patent on the phosphorylation sites identified and the participation of Grb10 in the feedback loop was filed on 9/23/2010 (no. 61/403,932 to J.B., S.P.G. and Y.Y.).

Supporting Online Material

www.sciencemag.org/cgi/content/full/332/6035/1322/DC1
Materials and Methods
SOM Text
Figs. S1 to S6
Tables S1 to S3
Databases S1 to S5
References

25 October 2010; accepted 22 April 2011
10.1126/science.1199484